Localized electrochemical impedance for characterizing welded areas of dissimilar Al alloys 2024-T3 and 7475-T761 joined by FSW

C. P. DE ABREU[1], I. COSTA[2], H.G. DE MELO[3], N. PÉBÈRE[4], V. VIVIER[5]

[1]*Instituto de Pesquisas Energéticas e Nucleares, Brazil, caioabreu5@gmail.com*
[2]*Instituto de Pesquisas Energéticas e Nucleares, Brazil, icosta@ipen.br,*
[3]*Universidade de São Paulo, Brazil, hgdemelo@usp.br*
[4] *Université de Toulouse, France, nadine.pebere@ensiacet.fr*
[5]*LISE-CNRS-UMR 8235, Université Pierre et Marie Curie, France, vincent.vivier@upmc.fr*

Abstract

Friction Stir Welding (FSW) is an efficient way to join high strength aluminum alloys avoiding defects that are usually found when conventional techniques are adopted. The aeronautic industry has shown great interest in this welding method, either for joining similar or dissimilar alloys. However, FSW generates different microstructural areas that could give rise to galvanic couplings on the welding area. In the present study, FSW was used to join two similar and dissimilar aluminum alloys, the AA2024 and the AA7475 alloys. To evaluate the effect of the welding process on the corrosion resistance of the joined alloys, electrochemical impedance spectroscopy studies, either global or localized (LEIS), have been carried out in a low corrosive medium (0.1 M Na_2SO_4) or with a small addition of chlorides (0.1 M Na_2SO_4 + 0.001 M NaCl). A gel visualization technique was also employed to detect possible galvanic couplings of the different zones formed during the FSW welding. OCP measurements were also performed on both individual aluminum alloys and on the zones affected by FSW. LEIS investigations were performed at different locations above the different microstructural zones induced by the FSW process on both alloys. Galvanic coupling was clearly evidenced at the interface between the two alloys, contrary to the results reported in literature for the welding of similar alloys, for which no galvanic coupling was evidenced.

Keywords: Friction Stir Welding, Aluminum Alloys, FSW of dissimilar alloys, Galvanic coupling.

Introduction

Research in the area of technological developments in the aircraft industry has been mainly focused on the weight reduction and durability increase of the parts used in aircrafts that lead to long lifetime, reduced amount of repairs, and fuel consumption as well as the decrease of emission of harmful gases in the atmosphere. There are two main ways for reducing the aircraft weight. The first is the reduction material density, for instance by replacing some of the material used by lighter ones. The second is the use of new welding techniques to substitute rivets used for joining overlay sheets. Industry experts thus estimate that the reduction of the overall weight of aircrafts by the two main ways specified above can reach 15% [1].

The conventional welding techniques that result in melting process are not effective for high strength aluminum alloys, including the alloys of the 2xxx and 7xxx series. These techniques lead to defects formed due to differences between thermal expansion coefficients of solidified regions and the liquid phase film. This film composition is similar to the eutectic, resulting in a number of cracks in the final stage of weld solidification besides great difference in the mechanical strength between the base metal and the welded joint. In order to solve this problem, T. Wayne from the TWI (The Welding Institute) in England, developed in 1990 and patented in 1991, the welding process known as Friction Stir Welding (FSW). In this process, welding occurs in the solid state resulting in less distortion and reducing the change of mechanical properties. However, the FSW process leads to heterogeneities at the surface and four zones of distinct microstructures, namely the nugget zone, the thermomechanically affected zone (TMAZ), the heat affected zone (HAZ), and the base metal (BM). Direct contact between two of these different zones induces galvanic coupling at their interfaces when a corrosive environment is present leading to corrosion processes at their surfaces. This is particularly true when alloys of different chemical composition are joined by FSW process.

Several studies have investigated the FSW effect on mechanical properties of the materials, microstructure and corrosion evolution as a function of time [3-5]. Local electrochemical techniques have been used to study the influence of the FSW process on the localized corrosion resistance of dissimilar alloys joined by this type of process [2].

Bousquet *et al.* (2011) [6] studied the relation between the microstructure of the AA2024-T3 alloy welded by FSW and the electrochemical behaviors associated to the second phase particles, as well as the effect of FSW process parameters on the localized corrosion susceptibility of this aluminum alloy. They found that the HAZ near to the TMAZ was preferentially corroded. Other works have also investigated the effect of the different zones generated by FSW of the AA2024-T3 alloy on its corrosion resistance [7,8]. The electrochemical potentials measured at the various zones of different microstructure created by the FSW process showed that the lowest potentials were associated to the nugget area. Lumsden *et al.* (2003) [9] studied the influence of FSW process on the corrosion properties of the AA7050-T7651 alloy and showed that the interface between the nugget zone and the TMAZ was preferentially corroded.

The literature shows that the microstructure modifications that arise from the use of FSW process favors the creation of galvanic coupling between the different zones formed by the FSW welding process and also suggest that it depends on the process parameters adopted.

Some groups have also investigated the corrosion susceptibility of dissimilar alloys welded by FSW, such as the welding of Al/Cu alloys [10,11], Al/Mg alloys [12] and different aluminum alloys [13,14].

It is known that the AA2024 alloy has two types of intermetallic particles, which play a major role in the degradation processes of the alloys: Al_2CuMg (S phase) and particles containing Fe [15,16,17], where the intermetallic Al-Cu-Mg are attacked in the first instants of immersion by aggressive solution, as well as intermetallic Al-Cu-Fe alloy prevailing in 7475 alloy [18,19,20].

Lacroix *et al.* (2009) [21] and Blanc *et al.* (2010) [22] investigated the galvanic coupling between Al and Cu by means of local electrochemical impedance spectroscopy technique (LEIS). This technique was proven to be extremely useful for describing the galvanic coupling between two adjacent areas, for instance the difference in behavior between the various microstructural zones formed by FSW welding of 2xxx with 7xxx alloys [7]. It was also found to be valuable in the analysis of the of Al-Cu /Al-Cu-Mg alloy model to simulate the electrochemical behavior of Al_2CuMg particles in contact with the AA2024 aluminum alloy matrix [23].

The aim of the present study was to evaluate the effect of the welding process on the localized corrosion resistance of dissimilar Al alloys joined by FSW. Localized electrochemical impedance spectroscopy (LEIS) studies have been carried out in a low corrosive medium (0.1 M Na_2SO_4) to which a small amount of chlorides (0.001 M NaCl) was also added.

Materials and methods

Materials

The materials investigated in this study were the AA2024-T3 and AA7475-T761 alloys, joined by FSW. The assembly was provided by EMBRAER as 2.0 mm sheets. The chemical compositions of the alloys are shown in Table 1.

Table 1. Chemical composition (wt. %) of the aluminum alloys studied.

	AA2024-T3	**AA7475-T761**
Element	(%)	(%)
Al	92.3 ± 0.5	89.4 ± 0.5
Mg	1.6 ± 0.2	1.9 ± 0.2
Si	0.19 ± 0.02	0.15 ± 0.02
P	0.03 ± 0.01	0.03 ± 0.01
S	0.02 ± 0.01	0.05 ± 0.01
Ca	0.04 ± 0.01	0.06 ± 0.01
Ti	0.05 ± 0.01	0.04 ± 0.01
Cr	0.04 ± 0.02	0.22 ± 0.01
Mn	0.64 ± 0.06	0.02 ± 0.01
Fe	0.22 ± 0.01	0.12 ± 0.02
Cu	4.8 ± 0.5	1.7 ± 0.2
Zn	0.08 ± 0.01	6.2 ± 0.6

Methods

The aluminum alloys microstructures were observed by optical microscopy after etching for 30 seconds with Keller's reagent.

The corrosion resistance of the dissimilar aluminum alloys welded by FSW was evaluated in 0.1 mol L^{-1} Na_2SO_4 with or without 0.001 mol L^{-1} NaCl solution. The electrochemical behavior of the AA2024-T3, AA7475-T761 aluminium alloys, either individually or at the FSW welded zones was monitored as a function of exposure time to the electrolyte by measuring the open circuit potential (OCP) during 8 h, and by using electrochemical impedance spectroscopy (EIS). The EIS tests were performed using a a Solartron 1287 Potentiostat and a Solartron 1250 frequency response analyzer. The applied potential sine-wave perturbation was 20 mV (rms) and the measuring frequency ranged from 63 kHz to 10 mHz. A three-electrode setup configuration was used for the EIS tests with the aluminum alloys with an exposed area of 3.1 cm^2 as working electrode, an Ag/AgCl, 3M KCl electrode as reference and a platinum wire as the auxiliary electrode.
A gel visualization technique was employed to detect possible pH variations ascribable to galvanic couplings between the dissimilar alloys welded and their different zones formed by FSW welding. The gel was prepared by mixing 3 g of agar-agar with 5 mM NaCl and 15 mL of universal indicator in 100 mL of water heated at 100 °C. The gel was subsequently laid on the FSW sheet as a thin layer of 1–2 mm thickness. Color modifications due to pH changes allowed identifying the anodic and cathodic regions across the cross section areas of the weld.

LEIS measurements were performed with a Solartron 1287 Potentiostat, a Solartron 1250 frequency response analyzer, a high impedance input amplifier with a differential amplifier and a probe scanning assembly system. For these measurements, the probe consisted of a dual electrode (a sharp Pt tip surrounded by a Pt ring). The two electrodes were used as local potential sensors. The applied potential sine-wave perturbation was 30 mV (rms) and the measuring frequency ranged from 63 kHz to 1 Hz. The LEIS measurements were also performed in the test solution used for EIS. It should be noted that solution with low conductivity is commonly used for LEIS experiments to optimize the resolution of the measurement. The bi-electrode was positioned close to the working electrode surface and with the help of a stepper motors. Each measurement was performed at 1 mm distances, following the sense of the AA2024-T3 alloy to the direction of AA7475-T761 alloy, through the weld region (FSW).

Results

Surface and microstructure characterization of the aluminum alloys welded by FSW

Figures 1 and 2 show a picture and optical micrographs of the different zones resulting from the FSW of the two dissimilar Al-alloys joined by FSW.

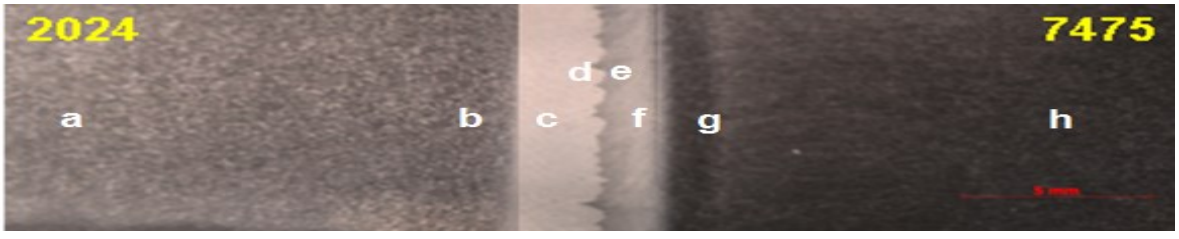

Figure 1. picture of the dissimilar AA2024-T3 and AA7475-T761 alloys joined by FSW showing: (a) MB ;(b) HAZ / TMAZ; (c) TMAZ; (d) nugget of AA2024-T3; and (e) nugget; (f) TMAZ; (g) HAZ / TMAZ; (h) MB of AA7475-T761 alloy.

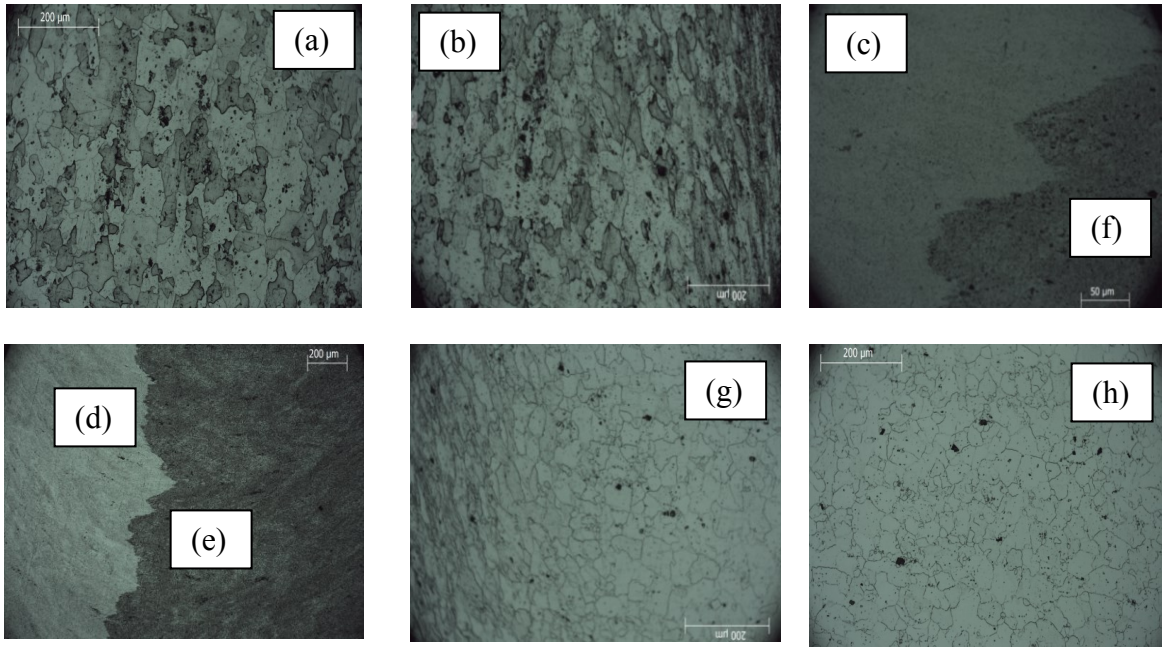

Figure 2. Optical micrographs of the various zones in the dissimilar AA2024-T3 and AA7475-T761 alloys joined by FSW showing: (a) MB; (b) HAZ/TMAZ; (c) TMAZ and (d) nugget of AA2024-T3; and (e) nugget; (f) TMAZ; (g) HAZ/TMAZ and (h) MB of AA7475-T761 alloy.

The grains in the nugget zones (Figure 2(d) (e)) were not revealed likely due to their tiny size caused by recrystallization provoked by the higher temperatures reached in this area. The microphaphs show that is hard to evidence the boundaries of the HAZ for both of the alloys. Similar microsctructures are shown in Figure 2(a) corresponding to the AA2024 alloy unaffected zone and the left end of 2(b), that corresponds to the HAZ of the AA2024 alloy. The same observation is valid for the AA7475-T761 alloy with the microstructure shown at the right end of Figure 2(g) that can be related to the HAZ of the AA7475-T761 alloy being similar to that shown in Figure 2(h) related to the AA7475-T761 unaffected zone. The TMAZ in both alloys are indicated by the deformed (elongated) grains due to plastic deformation resulting from the tool shoulder rotation against the alloy and the high temperatures reached during the process as shown at the right end of Figure 2(b) and left end of Figure 2(g). The clearly seen interface that separates the two alloys is typical of FSW of dissimilar alloys showing a clear distinction of the alloys brands. The large interface suggests high susceptibility to galvanic coupling at these zones.

Corrosion characterization of the aluminum alloys welded by FSW

Figure 3 shows the open circuit potential (OCP) measurements obtained for both alloys, individually and for the nugget zone during 8 h of exposure to the Na_2SO_4 (0.1 mol L^{-1}) + NaCl (0.001 mol L^{-1}) solution.

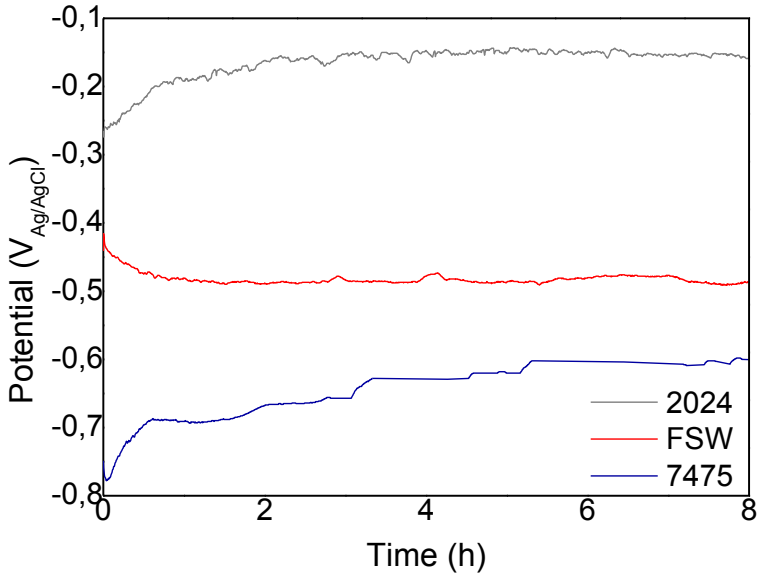

Figure 3. Open circuit potentials as a function of exposure time of the AA2024-T3 and AA7475-T761 alloys individually and at the nugget zone of the FSW joined dissimilar alloys. Na_2SO_4 (0.1 mol L^{-1}) + NaCl (0.001 mol L^{-1}) solution.

The results of Figure 3 show a fairly stable OCP after 2 hours of exposure to the electrolyte for the 3 samples. The OCP values corresponded to approximately -0.2 V (Ag/AgCl) for the AA2024-T3 alloy and nearly -0.65 V (Ag/AgCl) for the AA7475-T761 alloy. At the nugget zone, the OCP stabilizes at -0.5 V(Ag/AgCl), which is between the two other values, but closer to the AA7475-T761 one. These results indicate galvanic coupling when the alloys are welded by FSW, with a cathodic polarization of the AA2024-T3 alloys whereas the AA7475-T761 alloy is anodically polarized, which may result in a very active interface between these two alloys.

The evolution of the impedance response of the two aluminum alloys individually and for the nugget zone (indicated by FSW) during the first 8 hours of exposure to the test solution is shown in Figure 4 (Nyquist diagrams).

At 2 hours of exposure to the solution, the impedance modulus for the two alloys are similar and values of approximately 40 KΩ cm^2 are obtained for both alloys. However, the evolution of the electrochemical behavior of the AA2024-T3 alloy with time shows that impedance modulus decreases, whereas it increases for the AA7475-T761 one. Therefore, after 8 hours of exposure to the electrolyte, the electrochemical behavior of the two alloys are significantly different. For the nugget zone, much lower impedances were obtained likely due to galvanic coupling between the two alloys in close contact within this region. This result is in agreement with a most active region of the welded system.

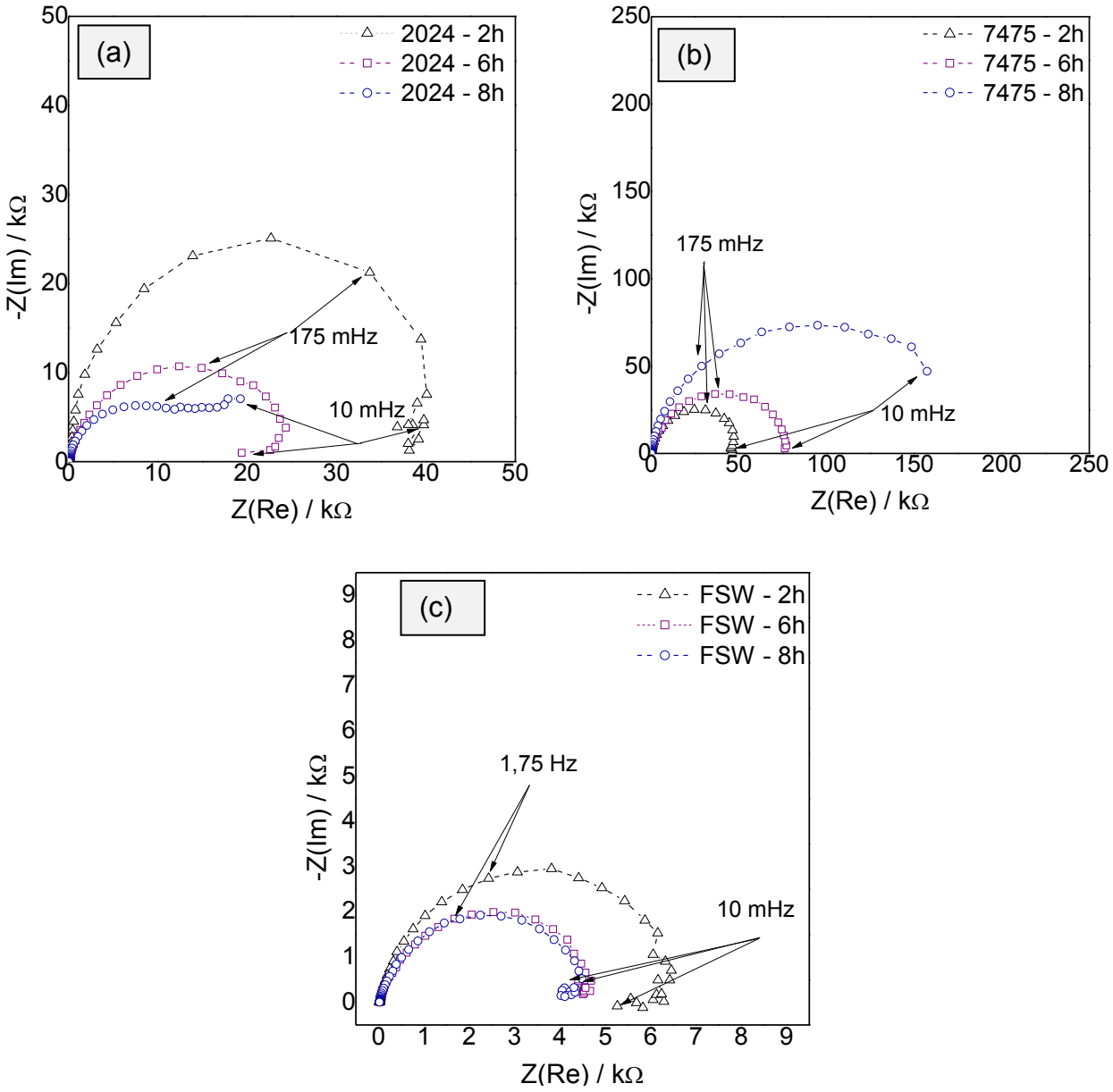

Figure 4. Nyquist diagrams obtained at various periods of exposure of the (a) AA2024-T3 alloy, (b) AA7475-T761 alloy and (c) nugget zone in 0.1 M Na_2SO_4 + 0.001 M NaCl solution

Figure 5 shows the effects of corrosion reactions on the surface pH of the AA2024-T3 and AA7475-T761 alloys welded by FSW during exposure to the agar-agar solution for a period of 8 hours. The main objective of this test was to macroscopically identify the most susceptible regions to corrosion of the two alloys, and the experimental procedure was based on previous published studies [8,24]. The color changes due to pH changes are used to identify anodic and cathodic regions across the cross section of the weld. Anodic regions become orange owing to acidity generated by aluminum cations hydrolysis, whereas cathodic regions become green due to the alkalinity caused by the oxygen reduction reaction.

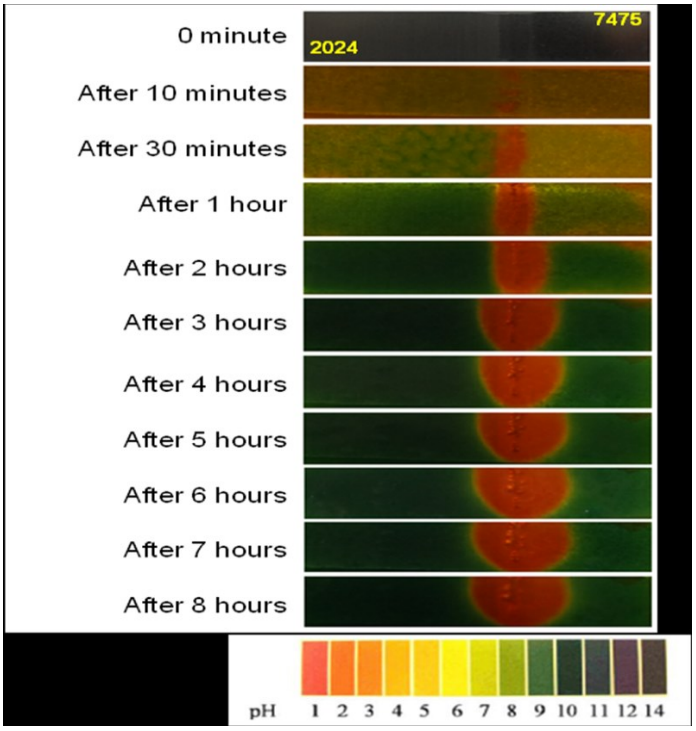

Figure 5. Agar-agar test results of the dissimilar alloys AA2024-T3 and AA7475-T761 joined by FSW process. Cross section region.

After 10 minutes of test, there is no clear color distinction between the various regions across the weld, and the film shows a homogeneous coloration. However, after 30 minutes, a clear color distinction had been established with the orange color being seen on the nugget /TMAZ zones on the AA7475-T761 alloy, showing that the anodic activity starts to develop on this region. This is more clearly seen for longer periods of test when the orange color spread to the adjacent zones, but always above the 7475-T761 alloy. Bubbles were seen at the anodic region after 2 hours and longer periods of test, associated to hydrogen evolution due to the high acidity resulting of hydrolysis stimulated by aluminum cations. The gas evolution was associated to the TMAZ of the 7475-T761 alloy.

Local electrochemical impedance spectroscopy (LEIS) tests were carried out in 0.1 mol L^{-1} Na_2SO_4 solution at various positions along a welding line, according to the positions of the probe (bi-electrode) schematically illustrated in Figure 6. The distance between two consecutive points corresponded to 1 mm. It is noteworthy that the addition of small amounts of chloride ions may adversely affect the resolution at high frequency range interfering with the evaluation of possible galvanic coupling. Consequently, for the LEIS tests, the solution was only composed of sodium sulfate. The first LEIS data were obtained after 2 hours of immersion and then after 6 and 8 hours of exposure. Each point indicated in Figure 6 was tested in sequence, and all the FSW affected and unaffected zones were contemplated.

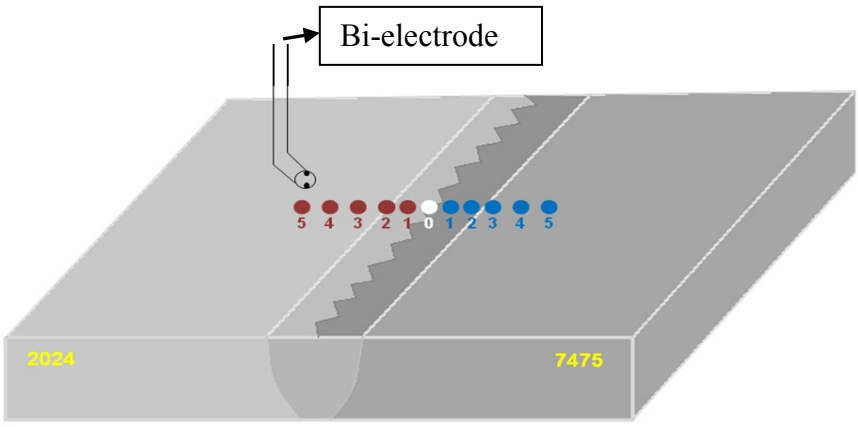

Figure 6. Bi-electrode placement scheme showing the points analyzed by LEIS through the AA2024-T3 and AA7475-T761 alloys welded by FSW.

Global impedance spectra were also measured during the 44 hours of the exposure of the whole FSW affected and unaffected zones to 0.1 mol L^{-1} Na_2SO_4 solution, and the results are shown in Figure 8. It is important to note that impedance decreased during the whole test period (44 hours). The literature reports inhibiting effects of sulfate ions for aluminum alloys [28,29]. However, in the present study, the impedance results indicated the attack of the sulfate solution to the surface film. This could be due to the galvanic coupling between the two alloys. Besides, it is likely that the passive film formed on the FSW affected zones is less resistant than that formed on the aluminum unaffected zones. Figure 7 shows macrographs of the dissimilar alloys AA2024-T3 and AA7475-T761 welded by FSW, prior to and after 24 hours of immersion. It shows that the AA2024-T3 alloy has been attacked (cathodic attack) whereas some tiny dark spots are seen on the AA7475-T761 alloy.

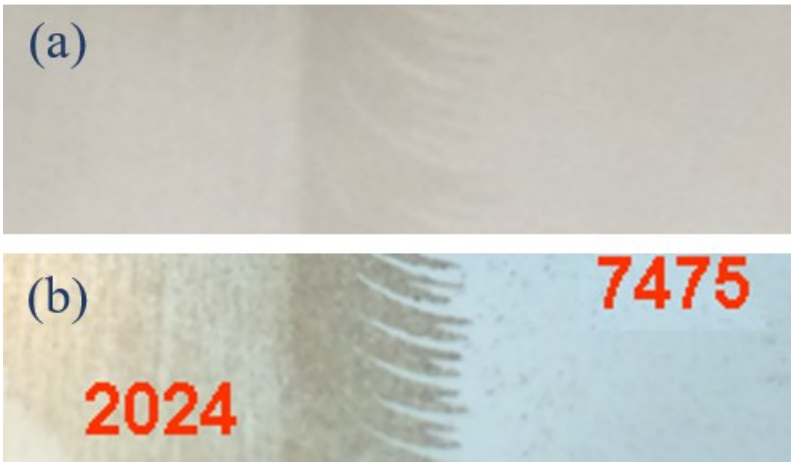

Figure 7. Macrographs of the dissimilar alloys AA2024-T3 and AA7475-T761 welded by FSW (a) prior to immersion and (b) after 24 hours of immersion in 0.1 mol L^{-1} Na_2SO_4 solution

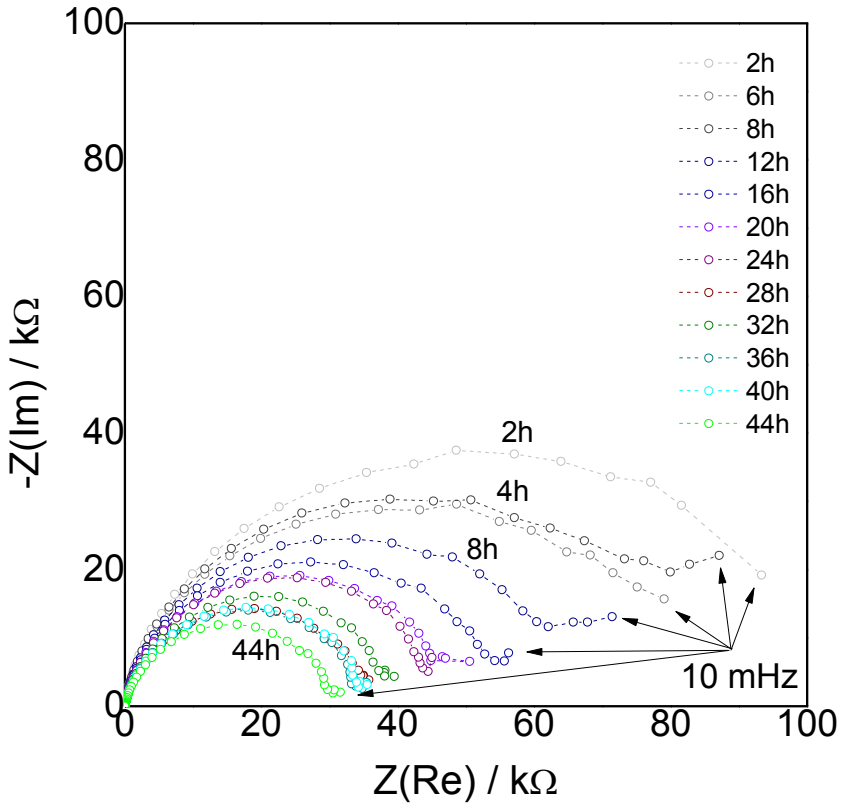

Figure 8. Global electrochemical impedance spectroscopy of the dissimilar alloys AA2024-T3 and AA7475-T761 welded by FSW for 44 hours of exposure to 0.1 mol L^{-1} Na_2SO_4 solution.

LEIS results obtained after 2, 6 and 8 hours of exposure to 0.1 mol L^{-1} Na_2SO_4 solution at the various locations indicated in Figure 6, along with the potential measured immediately after test initiation, are shown in Figure 9 in Nyquist representation. It is important to emphasize that the low frequency limits analyzed in the LEIS tests are higher (1 Hz) than those of the global impedance (10 mHz) due to the bi-electrode geometry and electrical noise.

The results in Figure 9 show some interesting aspects at the high frequency range. The high frequency region of the diagrams show the onset of an inductive loop which have been associated with galvanic coupling in model alloys by other authors [22,23,27]. This feature is more relevant the closest the probe is placed near the welded interface, that is, as the bi-electrode approaches the interface between the dissimilar aluminum alloys. This observation is contrasted by results obtained on the welding for similar alloys realized by the group that did not show any galvanic coupling. The presence of inductive loop at high frequencies has been attributed in literature to the geometric effect caused by distribution of equipotential line across the electrode surface [22,25,26].

The inductive loops observed at high frequency are more evident for shorter test periods (2 h) and tend to disappear at longer exposure times (6 h and 8 h). This could be due to the increasingly growth of the passive film and the inhibiting effect of sulfate ions on aluminum alloys with exposure time to the low aggressiveness electrolyte used, a contribution of precipitation of corrosion products blocking the surface of the corroded zones also cannot be ruled out.

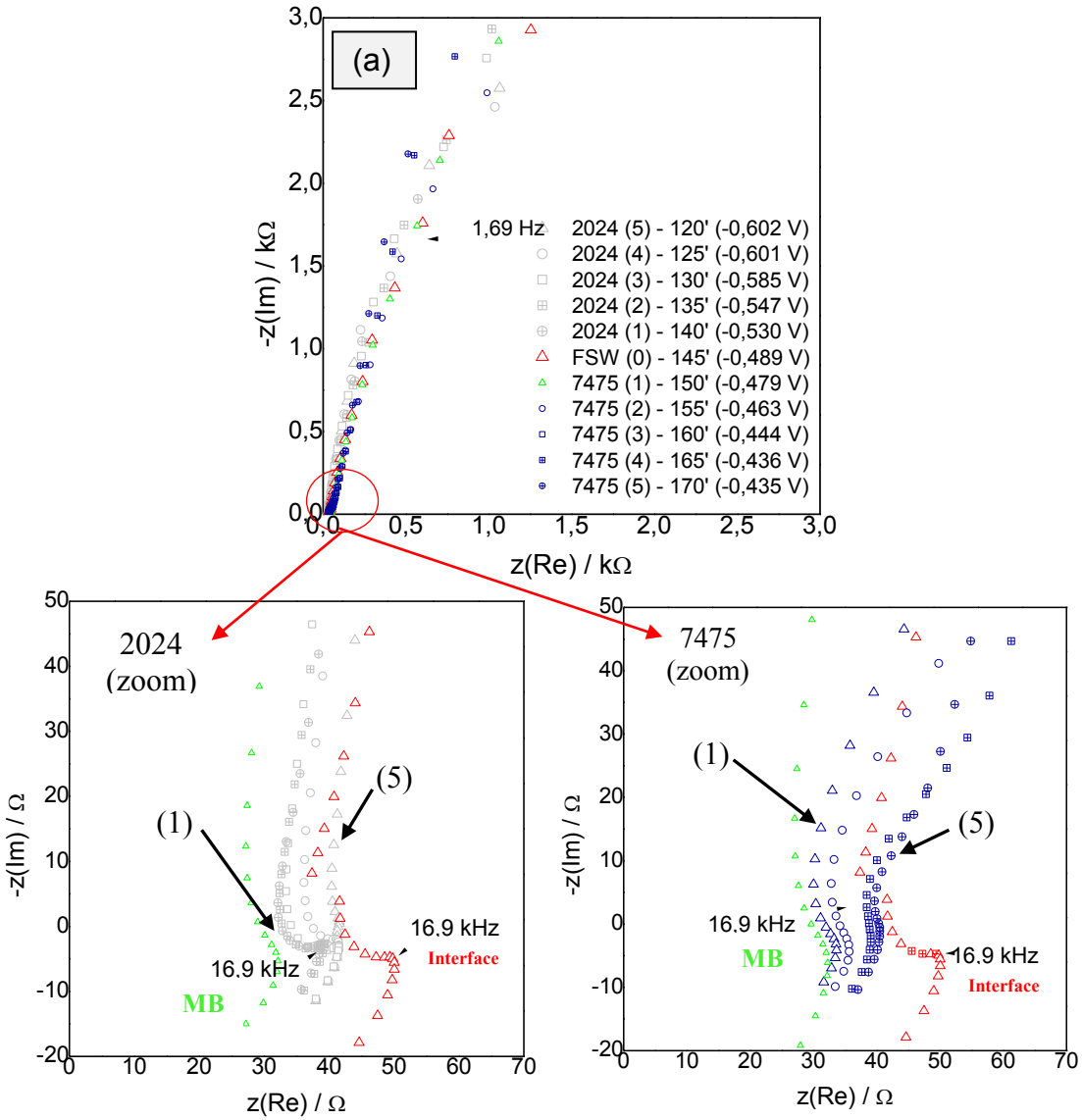
(a)
1,69 Hz
2024 (5) - 120' (-0,602 V)
2024 (4) - 125' (-0,601 V)
2024 (3) - 130' (-0,585 V)
2024 (2) - 135' (-0,547 V)
2024 (1) - 140' (-0,530 V)
FSW (0) - 145' (-0,489 V)
7475 (1) - 150' (-0,479 V)
7475 (2) - 155' (-0,463 V)
7475 (3) - 160' (-0,444 V)
7475 (4) - 165' (-0,436 V)
7475 (5) - 170' (-0,435 V)
-z(Im) / kΩ
z(Re) / kΩ
2024
(zoom)
(1)
(5)
16.9 kHz
MB
16.9 kHz
Interface
-z(Im) / Ω
z(Re) / Ω
7475
(zoom)
(1)
(5)
16.9 kHz
MB
16.9 kHz
Interface
-z(Im) / Ω
z(Re) / Ω

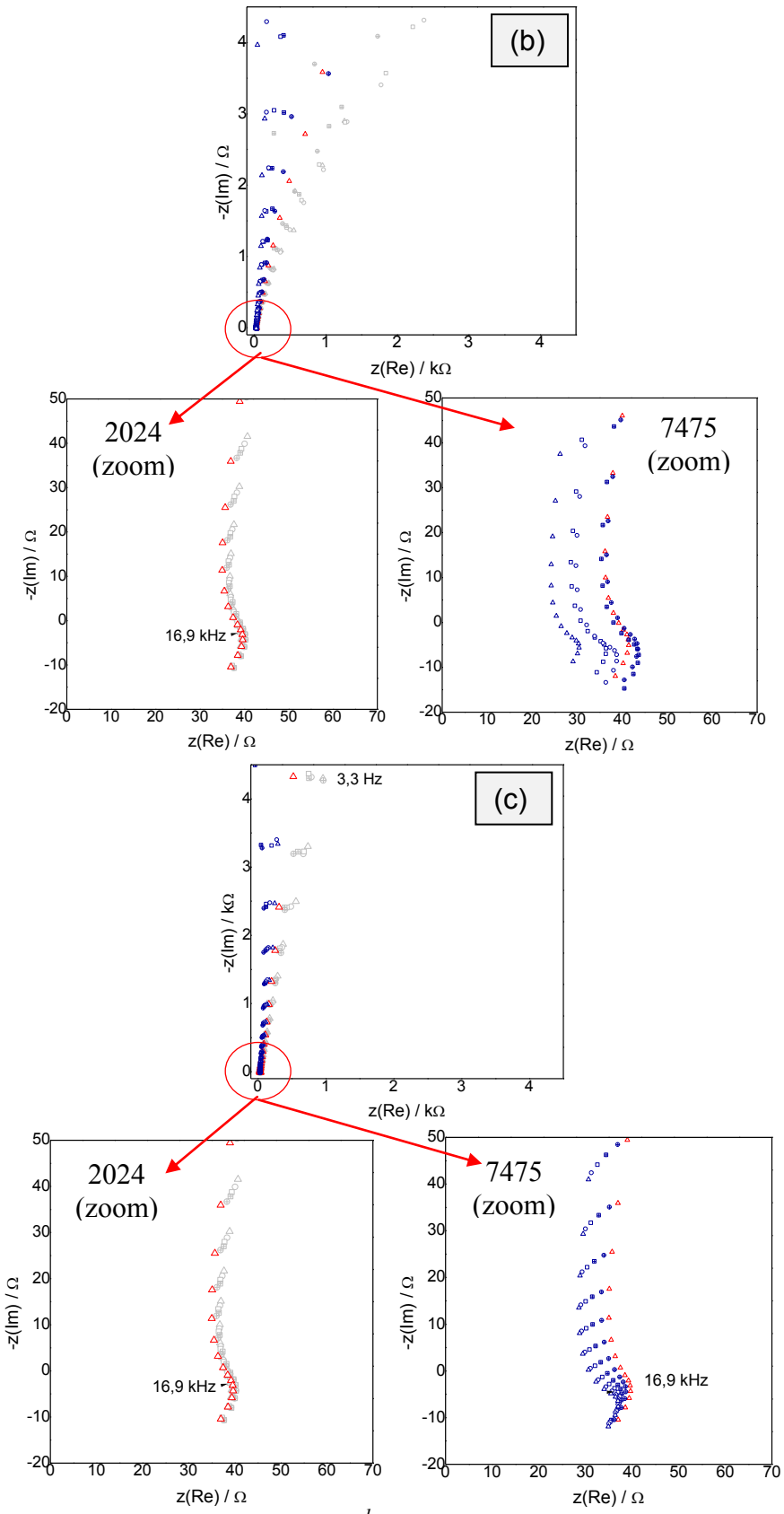

Figure 9. LEIS data obtained in 0.1 mol L^{-1} Na_2SO_4 solution at various points along a line starting from the matrix of the AA2024-T3 passing through the HAZ, TMAZ, nugget and then the same corresponding zones for the AA7475-T761 alloy after welding by FSW, for (a) 2 h, (b) 6 h and (c) 8 h of immersion.

Jorcin *et al*. [27] tested the galvanic coupling between pure Al and Cu after one hour exposure to 10^{-3} M Na_2SO_4 solution by LEIS. They found inductive loops which were dependent on the micro-electrode position and whose diameter was higher on the center of the Cu electrode. Lacroix *et al.* [23] carried out a theoretical approach of the results corresponding to the galvanic coupling of Al-Cu and Al-Cu-Mg alloys in 10^{-3} M Na_2SO_4 solution. It was observed that the inductive loops on the Al-Cu-Mg were larger when the probe was on the interface between the two alloys region (central welding), comparatively to the distant zones far from the interface, due to constriction of the potential field lines in this region. The same behavior of galvanic coupling was observed in this study at the interface, but mainly on the AA2024-T3 alloy (Figure 9-a – 2024 zoom).

Conclusions

This study investigated the corrosion behavior of two dissimilar aluminum alloys, AA7475-T761 and AA2024-T3, welded by FSW and the results showed that the first alloy behaves anodically relatively to the second one. Galvanic coupling was observed by LEIS when the probe was placed near the weld joint that is, as the bi-electrode approached the interface between the dissimilar aluminum alloys welded by FSW. The results of global EIS diagrams showed much lower impedances obtained when the exposed areas to the electrolyte contained the FSW affected zones comparatively to the two aluminum alloys tested individually.

References

[1] D. Dittrich,; J. Standfuss, J. Liebscher, B. Brenner, E. Beyer, Physics Procedia, **12** (2011) 113.

[2] CONNOLLY, B. J.; DAVENPORT, A. J.; JARIYABOON, M.; PADOVANI, C.; AMBAT, R.; WILLIAMS, S. W.; PRICE, D. A.; WESCOTT, A.; GOODFELLOW, C. J.; LEE, C.-M. Corrosion of a Dissimilar Friction Stir Weld Joining Aluminium Alloys 2024 and AA7010. ***Proc. 5th Int. Friction Stir Welding Symp.*** Metz, France, September 2004, TWI. 27

[3] MISHRA, R.S.; MA, Z.Y. Friction stir welding and processing, ***Mater. Sci. Eng***. R Rep. 50 (2005) 1–78.

[4] COLE, E.G.; FEHRENBACHER, A.; DUFFIE, N.A.; ZINN, M.R.; PFEFFERKORN, F.E.; FERRIER, N.J. Weld temperature effects during friction stir welding of dissimilar 6061-t6 and 7075-t6, ***Int. J. Adv. Manuf. Technol.*** 71 (2013) 643–652.aluminum alloys

[5] OUYANG, J.H.; KOVACEVIC, R. Material flow and microstructure in the friction stir butt welds of the same and dissimilar aluminum alloys, ***J. Mater. Eng. Perform***. 11 (2002) 51–63.

[6] BOUSQUET, A.; POULON-QUINTIN, A.; PUIGGALLI, M.; DEVOS, O.; TOUZET, M. Relationship between microstructure, microhardness and corrosion sensivity of an AA2024-T3 friction stir welded joint, ***Corrosion Science***, n 53, p 3026-3034, 2011.

[7] SIDANE, D.; BOUSAUET, E.; DEVOS, O.; PUIGGALI, M.: TOUZET, M.; VIVIER, V.; POULON-QUINTIN, A. Local electrochemical study of friction stir welded aluminium alloy assembly, Journal of Eletroanalytical Chemistry, v 737, p 206-211, 2015.

[8] JARIYABOON, M.; DAVENPORT, A.; AMBAT, R;. CONNOLLY, B.; WILLIAMS, S.; PRICE, D.The effect of welding parameters on the corrosion behaviour of friction stir welded. ***Corrosion Science***, n 49, p 877-909, 2007.

[9] LUMSDEM, J.; MAHONEY, M.; RHODES, C.; POLLOCK, G. Corrosion Behavior of Friction-Stir-Welded AA7050-T7651, ***Corrosion Science***, n 59, p 212-219, 2003.

[10] AKINLABI, E.T.; ANDREWS, A.; AKINLABI, S.A. Effects of processing parameters on corrosion properties of dissimilar friction stir welds of aluminium and copper, ***Trans. Nonferrous Met. Soc.*** China 24 (2014) 1323–1330.

[11] SARVGHAD-MOGHADDAM, M.; PARVIZI, R.; DAVOODI, A.; HADDAD-SABZEVAR, M.; IMANI, A. Establishing a correlation between interfacial microstructures and corrosion initiation sites in Al/Cu joints by SEM–EDS and AFM–SKPFM, ***Corros. Sci.*** 79 (2014) 148–158.
[12] STRASS, B.; WAGNER, G.; CONRAD, C.; WOLTER, B.; BENFER, S.; FÜRBETH, W. Realization of Al/ Mg-hybrid-joints by ultrasound supported friction stir welding — mechanical properties, microstructure and corrosion behavior, Adv. Mater. Res. 966–967 (2014) 521–535.
[13] SATHISH, R.; RAO, SESHAGIRI, V. Corrosion studies on friction welded dissimilar aluminum alloys of AA7075-T6 and AA6061-T6, Int. J. Electrochem. Sci. 9 (2014) 4104–4113.
[14] LARSON, D.; WALDERA, B.; SITTER, C.; KALITA, S. Microstructure and corrosion investigation of friction stir welds of dissimilar aluminum alloys, Mater. Sci. Technol. Conf. Exhib. 2011, MS T'11, vol. 2 2011, pp. 1546–1553.
[15] BLANC, C.; LAVELLE, B.; MANKOWSKI, G. The Role of Precipitates Enriched with Copper on the Susceptibility to Pitting Corrosion of the 2024 Aluminium Alloy. Mater. Sci. Forum, 1996, 217–222, 1559–1564.
[16] LIAO, C. M.; OLIVE, J. M.; GAO, M.; WEI, R. P. In-situ monitoring of pitting corrosion in aluminium alloy 2024, Corrosion, v 54, v 6, p 451-458, 1998.
[17] CAMPESTRINI, P.; VAN WESTING, E. P. M.; VAN ROOIJEN, H. W.; DE WIT, J. H. W. Relation between microstructural aspects of AA2024 and its corrosion behaviour investigated using AFM scanning potential technique. Corros. Sci., 2000, 42, 1853–1861.
[18] BLANC, C.; LAVELLE, B.; MANKOWSKI, G. The role of precipitates enriched with copper on the susceptibility to pitting corrosion of the 2024 aluminium alloy, Corrosion Science, v 39, n 3, p 495-510, 1997.
[19] BLANC, C.; GASTAUD, S.; MANKOWSKI, G. Mechanistic Studies of the Corrosion of 2024 Aluminium Alloy in Nitrate Solutions, Journal of the Electrochemical Society, v 150, n 8, p B396-B404, 2003.
[20] FERRARI, J. V.; DE MELO, H. G.; KEDDAM, M.; ORAZEM, M. E.; PEBERE, N.; TRIBOLLET, B.; VIVIER, V., Influence of normal and radial contributions of local current density on local electrochemical impedance spectroscopy. Electrochimica Acta, v 60, p 244-252, 2012.
[21] LACROIX, L.; BLANC, C.; PEBERE, N.; TRIBOLLET, B.; VIVIER, V. Localized Approach to Galvanic Coupling in an Aluminium-Magnesium System, Journal of the Electrochemical Society, v 156, n 8, p 259-265, 2009.
[22] BLANC, C.; PEBERE, N.; TRIBOLLET, B.; VIVIER, V. Galvanic couplign between copper and aluminium in a thin-layer cell, Corrosion Science, n 52, p 991-995, 2010.
[23] LACROIX, L.; BLANC, C.; PEBERE, THOMPSON, G. E.; N.; TRIBOLLET, B.; VIVIER, V. Simulating the galvanic coupling between S-Al2CuMg phase particles and the matrix of 2024 aerospace aluminium alloy, Corrosion Science, n 64, p 213-221, 2012.
[24] DONATUS, U. ; THOMPSON, G.E. ; ZHOU, X. ; WANG, J. ; CASSELL, A. ; BEAMISH, K. Corrosion Susceptibility of Dissimilar Friction Stir Welds of AA5083 and AA6082 Alloys. MaterialsCharacterization, 107, 85–97, 2015.
[25] HUANG, V. M.; VIVIER, V.; WU, S. L.; ORAZEM, M. E.; PEBERE, N.; TRIBOLLET, B., The Apparent Constant-Phase-Element Behavior of a Disk Electrode with Faradaic Reactions – A Global and Local Impedance Analysis. Journal of The Electrochemical Society, v 154, p c99-c107, 2007.
[26] HUANG, V. M.; WU, S. L.; ORAZEM, M. E.; PEBERE, N.; TRIBOLLET, B.; VIVIER, V., Local eletrochemical impedance spectroscopy: A review and some recent developments. Electrochimica Acta, v 56, p 8048-8057, 2011.

[27] JORCIN, J.; BLANC, C.; PEBERE, N.; TRIBOLLET, B. ; VIVIER, V. Galvanic coupling between pure copper and pure aluminium, Journal of the Electrochemical Society, v 155, p C46-C51, 2008.
[28] C. Blanc, B. Lavelle, G. Mankowski, Mater. Sci. Forum, **217** (1996) 1559.
[29] C. Blanc, B. Lavelle, G. Mankowski, Corros. Sci., **39** (1997) 495.

Acknowledgements: Acknowledgements are due to CAPES (Capes/Cofecub N^{o}.806-14) and FAPESP (Proc. 2013/13235-6) for financial support to this research.